Ilmenite as alternative bed material for the combustion of coal and biomass blends in a fluidised bed combustor to improve combustion performance and reduce agglomeration tendency

Eduardo Garcia, Hao Liu[1]

Faculty of Engineering, University of Nottingham, University Park, Nottingham, UK

Abstract

Co-firing coal and biomass has the potential to reduce GHG emissions. However, high levels of alkali and alkaline metals in biomass ash can bring additional issues to the operation of coal-fired boilers. This study investigates the effects of ilmenite as the bed material on CO and NO_x emissions and combustion efficiency of a coal and biomass blend, and the agglomeration tendency of the bed material with a pilot-scale (30 kWth) bubbling fluidised bed combustor. The experiments were carried out at 900 °C using a bituminous coal blended with wheat straw pellets at 40 wt% as the fuel and silica sand as the baseline bed material. Samples of agglomerates collected from the combustor and cyclone ash were characterised by SEM-EDS, XRD, and XRF. The results revealed that ilmenite could reduce the level of excess air required to achieve complete combustion due to lower CO emissions and less efficiency loss compared to silica sand. However, ilmenite increased NO_x emissions. Furthermore, the characterisation of the obtained agglomerates and cyclone ash showed that ilmenite could hinder the K-rich molten substance attachment to the bed material, leading to significantly smaller agglomerates and hence less tendency towards defluidisation in comparison to silica sand.

Keywords: Co-combustion of coal and biomass, ilmenite, fluidized bed combustion, agglomeration, combustion performance.

[1] Corresponding author: liu.hao@nottingham.ac.uk

1. Introduction

For decades fossil fuels have been the main energy source worldwide, contributing to over 80% of the total primary energy use worldwide in 2019 [1]. Coal is still the main resource for electricity and heat generation in many parts of the world such as India, China, and the United States. Coal combustion in the world power and heat generation sector accounted for 30% of all energy-related CO_2 emissions, exceeding 10 Gt CO_2 in 2018 [2]. The continued dominance of fossil fuels, particularly coal, in the world energy mix is largely due to the slow uptake of low-carbon technologies [3,4]. According to IEA [2], CO_2 emitted from coal combustion was responsible for over 0.3°C of the 1°C increase in global average annual surface temperatures above pre-industrial levels. This makes coal the single largest source of global temperature increase.

Co-combustion of coal and biomass is a promising alternative in the short-term for reducing the deleterious effect of coal use in the production of electricity and heat but it still faces unsolved challenges [5,6]. Co-combustion of biomass and coal in comparison to exclusive coal use leads to the reductions of greenhouse gas (GHG) and harmful emissions such as NOx, SOx, CO. Furthermore, co-combustion can lower the cost of biomass utilisation through adapting existing dedicated coal combustion facilities rather than building new dedicated biomass combustion facilities [7]. However, the maximum ratio of biomass in the fuel blend in most commercial co-combustion applications has been limited to 5 - 10 % (on an energy basis), although 20 % is currently feasible and more than 50 % is technically achievable [8,9]. Despite the potential for greater reductions in CO_2 and combustion-generated pollutant emissions with a higher biomass ratio in the biomass and coal co-combustion, the current inability to address operational challenges linked to the biomass properties and ash characteristics, for example, high levels of alkali and alkaline metals in the fuel ash and the lower ash melting point in comparison to coal ash, limits the increase of biomass ratio in co-combustion applications.

The combustion efficiency of solid fuels in a combustion process is largely depending on the contact of oxygen and fuels during the combustion process and the stability of the process [10]. The better the contact between the oxygen and fuels, the lower the excess air is required to achieve a high combustion efficiency. For a fluidised bed (FB) combustion process, better oxygen and fuel contact could also lead to even temperature distributions in the FB combustor/boiler, reducing the likelihood of hot spots and the risk of agglomeration, leading to further benefits of less emissions of NOx, SO_2, CO and lower levels of unburnt carbon in the ash [11–13]. Recently, ilmenite, an iron-titanium oxide natural mineral, was used in the investigation of a novel concept called oxygen carrier aided combustion (OCAC) in fluidised beds. It had been shown to have the potential to improve the combustion efficiency while alleviating/solving the ash related issues that were originated from the alkali and alkaline metals in the biomass ash [12]. Replacing the bed material, totally or partially, with a solid oxygen carrier could enhance the contact between the oxygen and fuel. In the oxygen-lean regions within a FB combustor/boiler, the oxygen carrier material may provide the required oxygen for combustion. The oxygen carrier mainly reacts with the volatiles released from the solid fuels into CO_2 and H_2O [14]. Other reactions that may occur in a lesser proportion are between char and the oxygen carrier [15]. The iron oxide in ilmenite has several oxidation states. When considering the different reduction degrees, the Fe_2O_3-Fe_3O_4 step is faster than the steps of Fe_3O_4-FeO and FeO-Fe [16]. In general, the reaction rate of Fe_2O_3 with different fuels decreases with the following order: H_2 > CO > CH_4 > solid fuels [14]. The direct reduction of iron oxides by solid fuels is very slow and iron oxides cannot directly release gas phase O_2 via oxygen uncoupling [12]. However, the reduction of Fe_2O_3 by solid fuels either in the presence or absence of CO_2/H_2O can be significantly enhanced by alkali metals [17]. Furthermore, more Fe_2O_3 can be reduced to FeO when Al_2O_3 is coupled to produce $FeAl_2O_4$,

which has a high oxygen transport capacity [14]. Biomass often contains higher amounts of moisture and volatiles compared to coal. When burning high volatile fuels the lateral mixing may be insufficient when using conventional bed material such as silica sand, resulting in a requirement of a large amount of excess air [18]. An oxygen carrier has the possibility to not only facilitate the distribution of heat in the combustor, as silica sand, but also to even out the oxygen distribution. This can consequently result in a decreased amount of excess air required and increase the combustion efficiency [18].

Thunman et al. [13] carried out OCAC combustion experiments on a 12 MWth circulating fluidised bed, using ilmenite as the additive (up to 40 wt%) to the bed material of silica sand and burning woody biomass fuels. Their results showed CO and NOx emissions were reduced by 80% and 30%, respectively, in comparison with the case of silica sand as the bed material, and the authors attributed these reductions in CO and NOx emissions to the addition of ilmenite to the bed [13]. Furthermore, there was a reduction in the accumulation of deposits on the heat exchange surfaces. Hughes et al. [19] investigated the use of ilmenite as an additive and alternative bed material to improve the combustion performance and sulphur capture in a 50 kWth pilot-scale fluidised bed combustor under atmospheric oxy-fuel combustion conditions using two Canadian coals. Their results showed replacing the silica sand bed material with ilmenite led to a reduction of CO emissions by up to 30% and 13% corresponding to the two coals used. The CO reduction was found to be more prominent at low oxygen concentration in the flue gas. Furthermore, no agglomeration of the ilmenite bed material was found during the experiments. Wang et al. [10] studied the combustion performance and NO emissions of wood char combustion in a small fluidised bed reactor at different air to fuel ratios with four oxygen carriers (ilmenite, manganese ore and two by-product oxides from steel production) and quartz sand as the bed materials. Their results showed the use of oxygen carriers as the alternative bed

material instead of the quartz sand led to an improvement in combustion efficiency and reduced CO emissions. The use of oxygen carriers as the bed material made it possible to decrease the excess air and, thereby, lower the NO emissions, while keeping the same level of CO emissions. The increase in combustion efficiency was attributed to the reactivity of the oxygen carriers with CO. Among the oxygen carriers under study, manganese ore showed better performance in improving combustion efficiency and reducing CO emissions. However, it agglomerated earlier than the other oxygen carrier during the combustion tests [10].

Agglomeration and defluidisation are the well-known operational issues associated with biomass FB combustion boilers/combustors [20]. The alkali metals in biomass ash can be readily vaporised due to being present in ionic forms or organically bound rather than associated with minerals [21]. The released alkali metals can interact with the bed material during thermal degradation. When silica sand is used as the bed material, the alkali metals from the biomass ash can react with silica forming low-melting silicates characterised by lower melting point temperatures than the individual components [22]. As a result, the sand particles are coated with a sticky surface that then grows to larger agglomerates [23,24]. Agglomeration with the bed material is a major problem that can be difficult to detect and can propagate to the whole bed resulting in an unscheduled shutdown for replacement of the bed material, adversely affecting the cost and reliability of the process [25–27]. The use of oxygen carrier materials as bed materials or additives in OCAC applications may impact the agglomeration and defluidisation tendency of the fuels to be burned. To the best of authors' knowledge, few have specifically investigated the agglomeration and defluidisation behaviour of a fluidised bed combustor co-firing coal and biomass blends using an oxygen carrier (e.g. ilmenite) as the bed material or as an additive to the bed material of silica sand.

So far, few have paid particular attention to the potential capture of alkali and alkaline metals by oxygen carriers in OCAC combustion investigations. Corcoran et al. [28] studied the physical and chemical changes in ilmenite under OCAC woody biomass combustion conditions. Their results revealed the segregation of iron to the surface and the enrichment of titanium in the particles core along with the inward migration of K into the particles. In addition, the ash formed a calcium-rich double layer on the particle surface, surrounding the iron layer, and there was the formation of KTi_8O_{16} as a consequence of the diffusion of K into the core of the particle. Through more recent combustion experiments, Corcoran et al. [25] also found that longer process times led to the formation of a calcium layer around the particle surface and the migration of calcium into the particle.

The focus of this study was the investigation of the effect of ilmenite on the most representative flue gas emissions (i.e. CO, and NOx), combustion performance and agglomeration tendency when it was used as the alternative bed material in the co-combustion of coal and biomass in a pilot-scale fluidised bed combustor. For comparison purposes, tests of co-combustion of the same coal and biomass blend were carried out with silica sand as the bed material.

2. Experimental

2.1 Fuels and materials

The bituminous coal used in this study was supplied by the Newark Factory, British Sugar plc in the UK as ‘washed singles’ with 90 wt% of the particle size within the range of 12.5 mm and 28 mm. The same coal was used by the Newark’s industrial-scale fluidised bed combustion boiler for producing animal feed by drying sugar beet pulp subsequent to the sugar extraction process. The wheat straw was supplied by Agripellets Ltd (UK) in the form of pellets with the average diameter of 6 ±0.25 mm and length of 25 ±5 mm. Table 1 shows the proximate and ultimate analyses of these fuels and their ash compositions. The bituminous coal and wheat

straw have a similar level of ash content (7.99 wt% and 6.23 wt%, respectively) but the coal ash is mainly composed of acidic oxides (SiO_2, Al_2O_3, and Fe_2O_3), accounting for more than 90 wt% of the total ash, whereas the wheat straw ash is enriched with SiO_2 and basic oxides (K_2O, and CaO), accounting for more than 88 wt% of the total ash. To prepare for the co-combustion tests, the received bituminous coal was crushed and screened into the particle size fraction of 12 – 20 mm due to the operational limitation of the screw fuel feeder of the bubbling fluidised bed combustion system used in this study. The fuel blend reported here corresponds to a blend ratio of wheat straw (STW) at 40 wt% in the bituminous coal (BC) - straw (STW) mixture.

Table 1. Proximate and Ultimate Analyses of the Fuels and Their Ash Compositions.

	BC[a]	STW
Proximate Analysis (wt%, dry basis)		
Ash[b]	7.99	6.23
Volatile Matter (VM)	38.57	76.31
Fixed Carbon (FC)[c]	53.44	17.46
Moisture (wt%, as received)	2.83	4.96
High Heating Value (HHV)[d] (MJ/kg)	31.69	17.41
Ultimate Analysis (wt%, dry - ash - free basis)		
Carbon	70.94	43.88
Hydrogen	5.28	5.96
Nitrogen	1.68	0.71
Sulphur	1.23	0.58
Oxygen[c]	20.87	48.87
Ash Analysis[d] (wt%)		
SiO_2	43.21	64.69
P_2O_5	0.27	2.82
Fe_2O_3	11.84	0.42
Al_2O_3	35.41	0.55
CaO	4.03	8.05
MgO	0.83	3.33
Na_2O	0.18	0.00
K_2O	0.90	16.18
SO_3	2.28	2.29
Cl	0.00	1.60
TiO_2	0.96	0.01

[a] (BC) bituminous coal, and (STW) wheat straw.

[b] the ashing temperature was 550 °C for wheat straw and 815 °C for bituminous coal according to BS/EN/ISO 18122:2015 and BS/ISO 1171:2010, respectively.

[c] by difference.

[d] measured in an IKA C5000 Bomb Calorimeter on as received basis.

[e] By X-ray Fluorescence (XRF) of the ashes generated from the coal and wheat straw.

The silica sand (Garside 14/25) was used as the reference bed material of this study. It had a grain size ranging from 0.6 mm to 1 mm, and a particle density of 2655 kg/m^3. The ilmenite used in this study was supplied by Titania A/S, Norway, and had a density of 3700 kg/m^3 and a grain size ranging from 0.6 to 0.75 mm. Detailed chemical analyses of the bed materials used in this study are given in Table 2.

Table 2. Chemical composition of bed materials (wt%, by XRF).

	Silica sand	Ilmenite
SiO_2	96.67	27.68
P_2O_5	<0.01	0.13
Fe_2O_3	2.4	22.56
Al_2O_3	0.33	10.32
CaO	0.01	3.81
MgO	<0.01	6.97
Na_2O	0.03	1.57
K_2O	0.01	0.53
TiO_2	0.03	25.74

2.2 Bubbling fluidised bed combustion system

All the experiments were carried out on a 30 kW_{th} bubbling fluidised bed (BFB) combustion system which mainly consists of the BFB combustor, the coal/biomass screw feeder, and the auxiliaries (fluidisation air fan, gas sampling and analysis, etc.) as shown in Figure 1. The BFB combustor was made of a high-grade stainless steel pipe (ASTM A-312) with a wall thickness of 7.11 mm, an internal diameter of 154 mm, and a height of 2000 mm. It is divided into three sections namely the plenum chamber, fluidised bed, and freeboard with corresponding heights

of 200, 750, and 1050 mm, respectively. The fuel feeding point is located in the freeboard section at a height of 1200 mm from the bottom of the BFB combustor. The gaseous combustion products together with the entrained fine particles (char, ash, and bed materials) leave the freeboard section at a height of 1880 mm from the bottom of the BFB combustor and enter the cyclone where the fine particles are removed and collected by the cyclone particulate container.

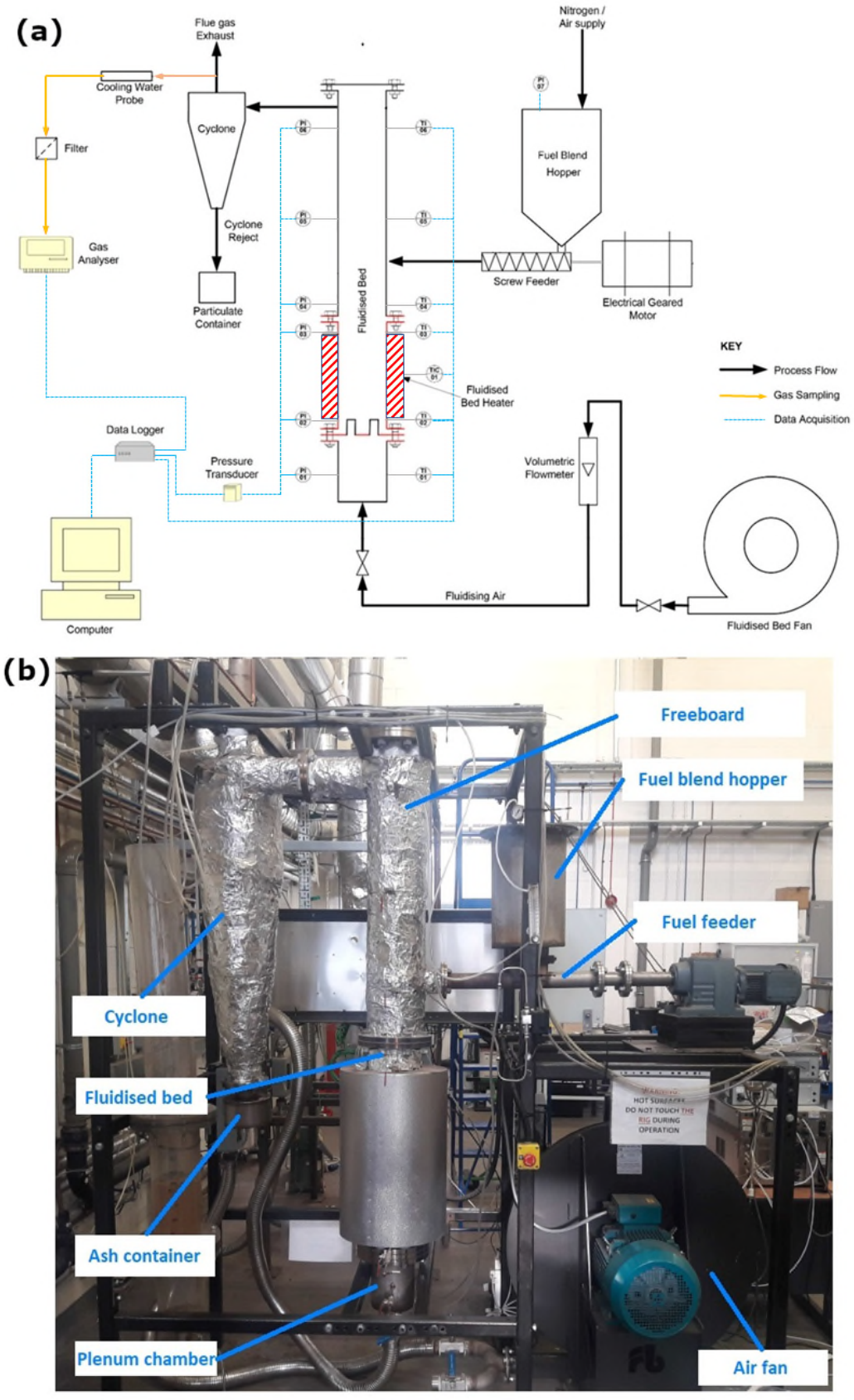

Figure 1. (a) Schematic diagram and (b) photo of the pilot-scale BFB combustion system [29].

Combustion air supplied by a centrifugal fan is used as the fluidisation air. It is controlled by the fan's rotational speed and a ball valve, monitored by a variable area volumetric air flow meter, and then fed into the combustor through a nozzle-type distribution plate [29]. The BFB combustor is surrounded by two semi-cylindrical ceramic electrical radiant heaters around the combustion bed section. The heaters are used to start the combustion process, providing the required heat to preheat the air flow and the bed particles before the onset of fuel feeding. The BFB combustor is equipped with a pressure transducer to measure the differential pressure across the dense bed region of the BFB combustor. 6 sheathed K-type thermocouples placed in the centre of the combustor/freeboard at different heights (i.e. 100, 300, 900, 1130, 1450, and 1770 mm from the bottom of the BFB reactor) are used to monitor the combustion temperature profile along the combustor height. Once the bed temperature reaches about 600 °C, the fuel feeding into the BFB combustor via the screw feeder can be initiated. The fuel feeding rate is controlled by the feeder motor inverter frequency according to the screw feeder calibration results.

2.3 Operating conditions

To minimise the interference of the difference in density between silica sand and ilmenite with the effect of bed materials to be investigated, the same value of minimum fluidisation velocity was used for both materials. The fluidisation number (U/ U_{mf}) was kept roughly constant by controlling the particle size to provide similar fluidisation conditions as shown in Table 3. The static bed height for all the experiments was set to 200 mm, corresponding to a bed inventory of 6.00 kg and 8.37 kg of silica sand and ilmenite, respectively.

Table 3. Operating parameters.

	Silica sand	Ilmenite
Particle density (kg/m^3)	2650	3700
Average size (range) (mm)	≈0.8 (0.6 – 1.0)	≈0.67 (0.6 – 0.75)
Minimum fluidisation velocity[a] U_{mf} (m/s)	0.23	0.22
Superficial gas velocity[a] U (m/s)	1.86	1.75
Bed height (mm)	200	200
Fluidisation number (U/U_{mf})	8.09	7.95
Fuel feeding rate (kg/h)	2.52 – 2.66	
Biomass blending ratio (wt%)	40	
Excess air (%)	87.4 – 112.5	
Bed temperature (°C)	900 ±5	
Fluidisation air flow rate (m^3/h)	38.4	

[a] at 900 °C.

During the experiments, the fuel feeding rate was finely adjusted to maintain the pre-set operating temperature, while the volumetric flow rate of the fluidising air, although always fluctuating to some extent due to low pressure air supply and fluidisation, was kept at the more or less same value of 38.4 m^3/h at ambient temperature and pressure (ATAP). A small flow of nitrogen (1.5 m^3/h @ ATAP) was fed to the fuel feeding hopper to prevent backfire and to stop the bed particles and hot gas flow entering the fuel feed line and hopper from the BFB combustor. Due to practical constraints (e.g. there was no heat removal from the combustor) and the interest to investigate the agglomeration tendency at high operating temperatures, the excess air was not optimised in this study.

The flue gas at the exit of the cyclone was continuously sampled and conditioned by means of water condensation traps and particulate filters. The cleaned gas sample was analysed by on-line gas analysers. O_2, CO_2, and CO concentrations were measured by an ABB Easy line continuous gas analyser (EL3020), whereas the NOx concentration was measured by a Horiba chemiluminescent NOx analyser (VA-3000). The output signals from the thermocouples, pressure transducer and the gas analysers were always continuously monitored and recorded

for the entire duration of each experiment using a DT80 DataTaker. It is worth noting that the current work focused on the most representative flue gas emissions, combustion performance, and fuel ash behaviour under the same operating temperature and fluidisation conditions.

2.4 Sample collection and analysis

After completing each experiment, the used bed material was visually inspected for signs of agglomeration. Samples of agglomerates, bed materials, and particles (mainly ash) in the cyclone particulate container were collected to be analysed by Scanning Electron Microscopy with dispersive X-ray microanalysis (SEM-EDX), X-ray fluorescence (XRF), and X-ray diffraction (XRD) techniques. Selected agglomerates samples were embedded in epoxy resin, then cut, polished, and coated with 10 nm carbon in order to obtain a cross-section of the particle to be analysed by SEM (FEI Quanta 600) equipped with EDX (Genesis 4000i X-ray analyser).

The composition of crystal phases of the agglomerates and the cyclone ash was analysed by XRF (Epsilon 3 XL High-performance benchtop spectrometer) and XRD (Bruker D8-Advance), respectively. Both the agglomerates and cyclone ash were ground to powder prior to the analysis. The extracted XRD profile took place with a capturing angle between 10° and 90° (2θ) and a step size of 0.02°/sec. In addition, the unburnt carbon in the cyclone ash samples was determined according to ASTM D7348 Standard Test Method for Loss on Ignition (LOI) of Solid Combustion Residues. After each experiment, the remaining fuel in the hopper was measured to double-check the fuel consumption and perform the determination of gaseous emissions (CO_2, CO, and NO_x) on an energy basis by the analysis of collected data from the gas analysers.

3. Results and discussion

3.1 Effect of ilmenite as alternative bed material on the axial combustor temperature profile

Figure 2 shows the axial temperature profile along the combustor height when ilmenite was used as bed material compared to silica sand. The results show that ilmenite enhanced fuel conversion in the dense bed region and less combustion took place in the freeboard in comparison to the silica sand bed. The use of an oxygen carrier as bed material can facilitate the combustion in the dense part of the bed and to some extent in the freeboard. Therefore, a more pronounce temperature drop for the experiments involving ilmenite was expected. Due to the interest to investigate the agglomeration tendency at high operating temperatures, the fuel feeding rate was finely adjusted to maintain the pre-set bed temperature (i.e. 900 °C) while the total combustion air flow rate was kept at the same value. This resulted in a slightly lower fuel feeding rate required to achieve the target temperature when ilmenite was used. The temperature profiles shown in Fig. 2 indicate that more heat was released in the dense bed when ilmenite was used as the bed material in comparison to the sand bed. This agrees with finding from Rýden et al. [30].

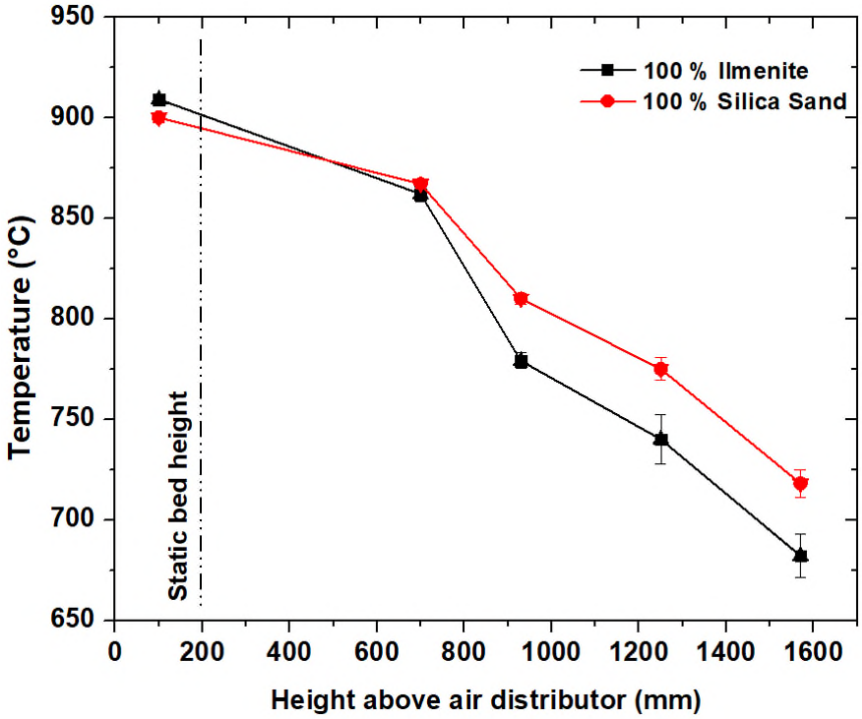

Figure 2. Temperature profile over the combustor. The dense bed temperature was in the range of 900 – 909 °C.

3.2 Effects of ilmenite as alternative bed material on CO, combustion performance, and NOx emissions

Figure 3 illustrates the reduction in CO emissions when ilmenite was used as the bed material in comparison to silica sand. This moderate level of reduction is attributed to the potential of oxygen carriers to increase the carbon conversion, which depends on the reactivity of the oxygen carrier with CO [10]. Similar results have been reported by Hughes et al. [19] and Wang et al. [10] using ilmenite as bed material. As bed material, ilmenite also had a positive effect on the reduction of unburnt carbon, increasing the combustion efficiency, which will be further discussed below. In addition, the effect of ilmenite on CO emissions has been reported to be greater at low excess air levels [19,30]. This is due to the fact that the rate of reaction of CO with gaseous oxygen is much faster than with the oxygen carrier and therefore when

oxygen is readily available, e.g. under high excess air levels as used in this study, the gaseous oxygen will control the overall rate of CO conversion [30].

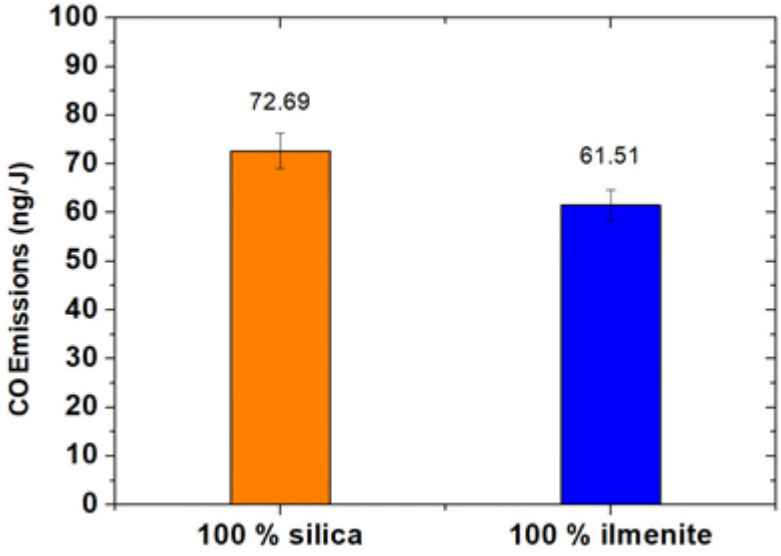

Figure 3. CO emissions: silica sand and ilmenite as bed materials.

The combustion performance was determined by the loss of efficiency due to unburnt carbon (UBC) in ash and CO emissions according to Kuprianov et al. [31] and Guo et al. [32], respectively.

$$Efficiency\ loss\ due\ to\ CO\ emissions = \left(\frac{CO}{CO_2 + CO}\right)100 \qquad (3)$$

where CO_2 and CO are the average concentration values in the flue gas during combustion experiments. Although there were some fluctuations during the course of the experiment, the measured results were stable as shown by the measured parameter profiles included in the supplementary material.

$$Efficiency\ loss\ due\ to\ UBC = \frac{32,866}{LHV}\left(\frac{UBC}{100 - UBC}\right)A \qquad (4)$$

where UBC is the unburnt carbon content in the ash in wt%. LHV is the low heating value of the fuel (i.e. coal and biomass blend). A is the fuel ash content in wt% on an as-received basis.

Figure 4 shows the efficiency losses due to unburnt carbon (UBC) and CO emissions for two different kinds of bed materials - silica sand and ilmenite. A reduced loss of efficiency was achieved when ilmenite was used as the bed material in comparison to silica sand. The reduction in CO emissions is attributed to the reaction with the oxygen carrier to CO_2. As mentioned in the introduction section, the decrease in unburnt carbon may be attributed to the reduction of Fe_2O_3 with solid carbon enhanced by alkali metals from the biomass ash. These results agree with the findings of Wang et al. [10], who found enhanced carbon conversions and higher combustion efficiency in their experiments using various oxygen carriers (i.e. ilmenite, manganese ore, and two oxide scales from the steel production industry) in a small fluidised bed reactor with wood char as fuel. Similar results were reported by Hughes et al. [19] who conducted combustion experiments under atmospheric and pressurised conditions in FBC systems using ilmenite and quartz sand as the bed materials burning two coals and found more profound effect of ilmenite on combustion performance under conditions of low excess air. Additionally, similar results were reported by Larsson et al. [33] and Lind et al. [34] who conducted experiments using ilmenite and silica sand to upgrade raw gas from biomass gasification.

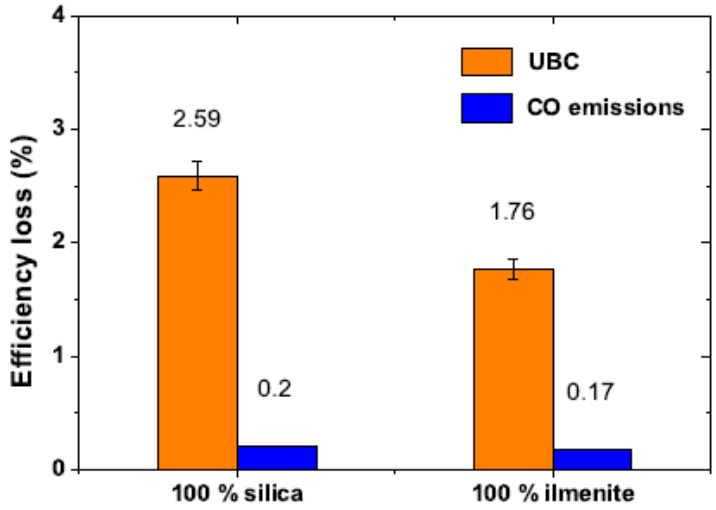

Figure 4. Comparison of silica sand and ilmenite as bed materials in terms of the losses of efficiency due to unburnt carbon (UBC) and CO emissions: the average CO emissions were

reported in Figure 3.

In co-combustion of coal and biomass, NOx emissions show a complicated pathway with the potential for less emissions than those from dedicated coal combustion [35]. The devolatilisation of bituminous coal produces mostly tarry compounds that at high temperatures decay rapidly to hydrogen cyanide (HCN) [36,37] . In contrast, biomass exhibits a nitrogen conversion behaviour closer to that of low-rank coals, forming mainly ammonia (NH_3), which may reduce NO to molecular nitrogen (N_2) (see Reactions 1 and 2) [7].

$$NH_3 + O_2 \rightarrow NO + H_2O + H \quad (1)$$

$$NH_3 + NO \rightarrow N_2 + H_2O + H \quad (2)$$

In fluidised bed combustion, the primary contributor of NOx is the fuel nitrogen [38–40]. In general, co-combustion leads to lower NOx emissions in comparison with coal combustion due to the lower nitrogen content of biomass, along with lower conversion rates of NH_3 to NO compared to HCN, the main product of coal fuel nitrogen [35,41]. The effect of ilmenite as bed material on NOx emissions is illustrated in Figure 5 which clearly shows the NOx emissions were higher when ilmenite was used as the bed material in comparison to the silica sand bed material. This is consistent with the findings of Wang et al. [10] and Hughes et al. [19], both of them had used ilmenite as their bed material with single stage air supply to burn coal and wood char, respectively. From Figures 3 and 5, it can be seen that the level of NOx emissions increased was accompanied by a reduction of CO emissions. This may suggest that the presence of ilmenite promotes NO formation by consuming reducing gas species (i.e. H_2 and CO), forming oxidising products (i.e. H_2O and CO_2). Oxygen carriers in the bed can lead to oxidising conditions in parts of the reactor that normally would be reducing [30]. In addition, it has been reported that oxygen carriers can enhance the conversion rate of ammonia (NH_3), leading to

higher levels of NO under Oxygen Carrier Assisted Combustion (OCAC) conditions [10]. This is particularly relevant for ilmenite due to the high content of Fe_2O_3, which has been shown to be able to oxidise NH_3 to form NO in experiments with different oxygen carrier materials [42].

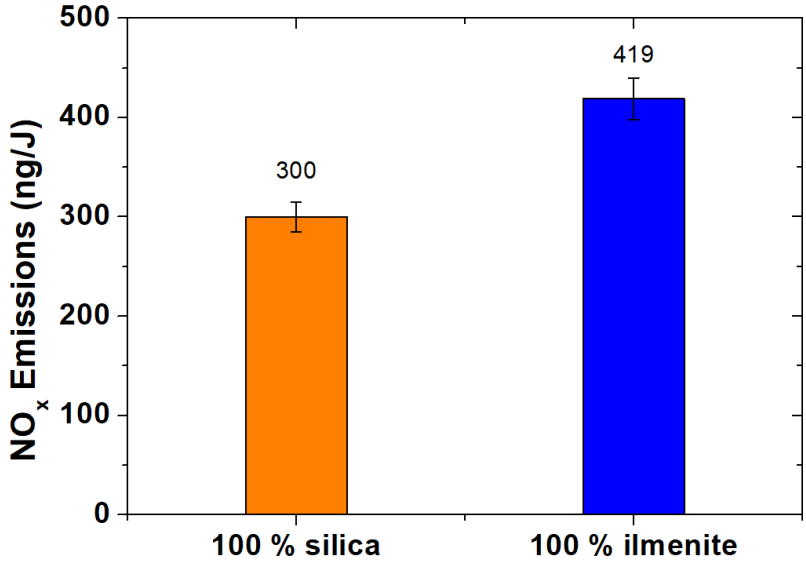

Figure 5. NOx emissions, ilmenite as bed material.

3.3 Effect of ilmenite as alternative bed material on agglomeration tendency

Although no evidence of defluidisation was observed during the 10 hours experiment in each case, the visual observation of the used bed material showed the existence of agglomerates in both cases (see Figure 6). Furthermore, the agglomerates formed from the same fuel blend under similar operating conditions were considerably less, smaller, and more fragile when ilmenite was used as the bed material in comparison to silica sand. Further sieve analysis of the used ilmenite bed material to quantify the fraction of agglomerates compared to the initial bed inventory showed to be unreliable due to the fragile nature of the agglomerates.

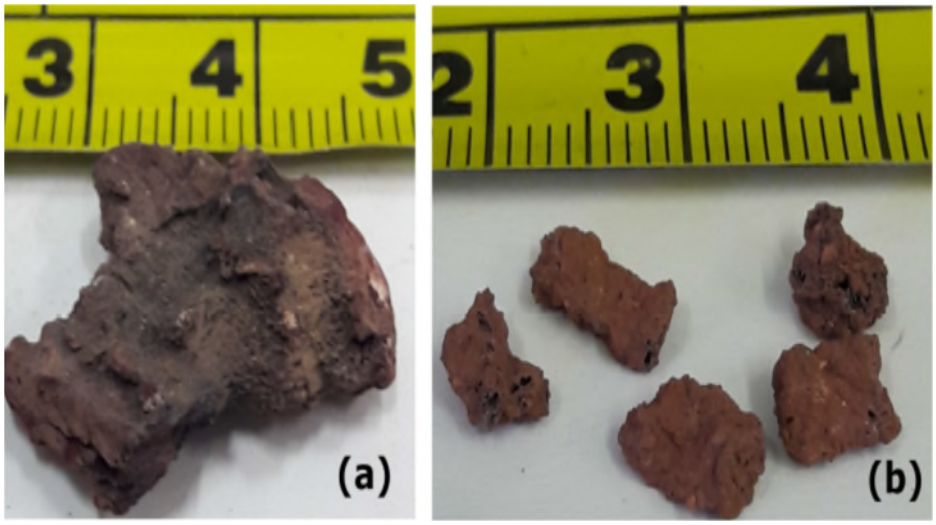

Figure 6. Comparison of samples of agglomerates produced from combustion of bituminous coal (BC) blended with wheat straw pellets (STW) at 40 wt% after 10 hours of operation using (a) silica sand, (b) ilmenite 100 wt% as bed materials (scale in cm).

As mentioned earlier, the agglomerates formed with the ilmenite bed appeared to be weak and could easily be broken into smaller pieces by hand. They have a porous structure which indicates the existence of a burning fuel particle inside, initiating the agglomeration process [43]. On the other hand, the agglomerates formed with the silica sand bed appeared to be completely fused as a result of heavy deposition and melting, without visible bridges connecting the particles. This suggests the formation of melts and later agglomeration along with the occurrence of intense sintering and secondary reactions after the agglomerates were initially formed tending to strengthen the agglomerates.

3.4 Characterisation of agglomerates from the bed and cyclone ash

3.4.1 Scanning Electron Microscopy coupled with Energy disperse X-ray Spectroscopy (SEM-EDS) of the agglomerates.

Figure 7 shows the SEM/EDX analysis of agglomerated bed materials using silica sand and ilmenite as the bed materials.

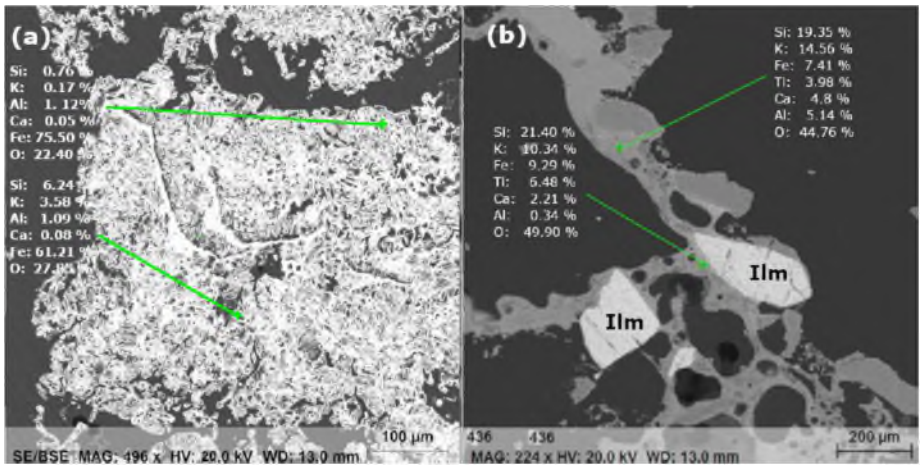

Figure 7. SEM/EDX micrograph showing the cross-sectional surface as well as the elemental spot analysis of the binder region of agglomerates (a) silica sand, and (b) ilmenite bed materials obtained from the combustion of BC blended with STW at 40 wt% after 10 hours of operation.

When silica sand was used as the bed material (see Figure 7a), a dense melt phase mainly composed of Fe with reduced amounts of Si, Al and K was observed. Similar findings were reported by Afilaka [29], who conducted coal combustion experiments in the same BFB combustor using the same silica sand bed material. It was reported that the iron content from the silica sand bed material could be responsible for the agglomeration formation due to the presence of FeO - Al_2O_3 - SiO_2 alkali silicates leading to the formation of melts and later agglomeration along with the occurrence of intense sintering. The oxidation of FeO or Fe to Fe_2O_3 with air has shown agglomeration of the particles [44]. Furthermore, the presence of Si and alkali metals could facilitate the sintering of iron oxides due to the formation of compounds with low melting points, such as potassium silicates and $FeSiO_4$ [14]. The agglomeration in fluidised bed combustion has been reported as a result of reactions involving iron oxides, silica minerals, and alkali metals, facilitated by localised reducing conditions within the combustor [45]. These localised reducing conditions may arise from either poor lateral bed mixing or oxygen-starved conditions near fuel feed locations. Further, during the iron oxide reduction in fluidised beds, the formation of iron whiskers has been reported as one of the main reasons for sticking phenomena leading to the defluidisation of the bed [46,47].

Agglomerates formed when ilmenite (Ilm) was used as the bed material showed the formation of binding bridges between the bed particles (see Figure 7b), with Si and K as the predominant elements in the binder. In addition, representative quantities of Fe, Ti, Ca and Al were found in the binder, suggesting the diffusion of these elements. It is widely accepted that these elements could react with K forming compounds with higher melting temperatures [48]. In fact, it has been reported that if the alternative bed material contains a sufficient amount of iron oxide (Fe_2O_3), the iron will react preferentially with alkali metals evolving to form $X_2Fe_2O_4$ (X represents either K or Na) which melts at a higher temperature of 1135 °C [49]. Furthermore, during straw combustion experiments using TiO_2 as an additive, a significant reduction of K vaporisation was reported by Wiinikka et al. [50]. Ilmenite is composed of different kinds of iron oxides as the active phases with some impurities (e.g. Al_2O_3 and TiO_2), which could serve as a natural support material to improve the mechanical properties while reducing the agglomeration tendency. In contrast to silica sand, when ilmenite is used as the bed material, FeO could react with Al_2O_3 and TiO_2 to produce $FeAl_2O_4$ and $FeTiO_3$, which not only prevent the sintering but also have a higher oxygen transport capacity [14].

The finding of this study suggests there were interactions between the ash components and the ilmenite. Similar results were found by Zevenhoven et al. [51], who reported a Fe and Ti rich phase in the bridges between particles during their experiments to investigate the influence of potassium-containing components on ilmenite bed material under oxidising conditions in a lab-scale fluidised bed reactor. To analyse the chemical composition of agglomerates and the binder linking the ilmenite bed particles, the EDX mapping technique was used and the results are presented in Figure 8. The distribution of Si, K, Ca, Al, Fe, Ti, and O across the surface of

the agglomerated bed material samples was identified as present. The intensity of the colour across a particular area indicates the extent of the element in that region.

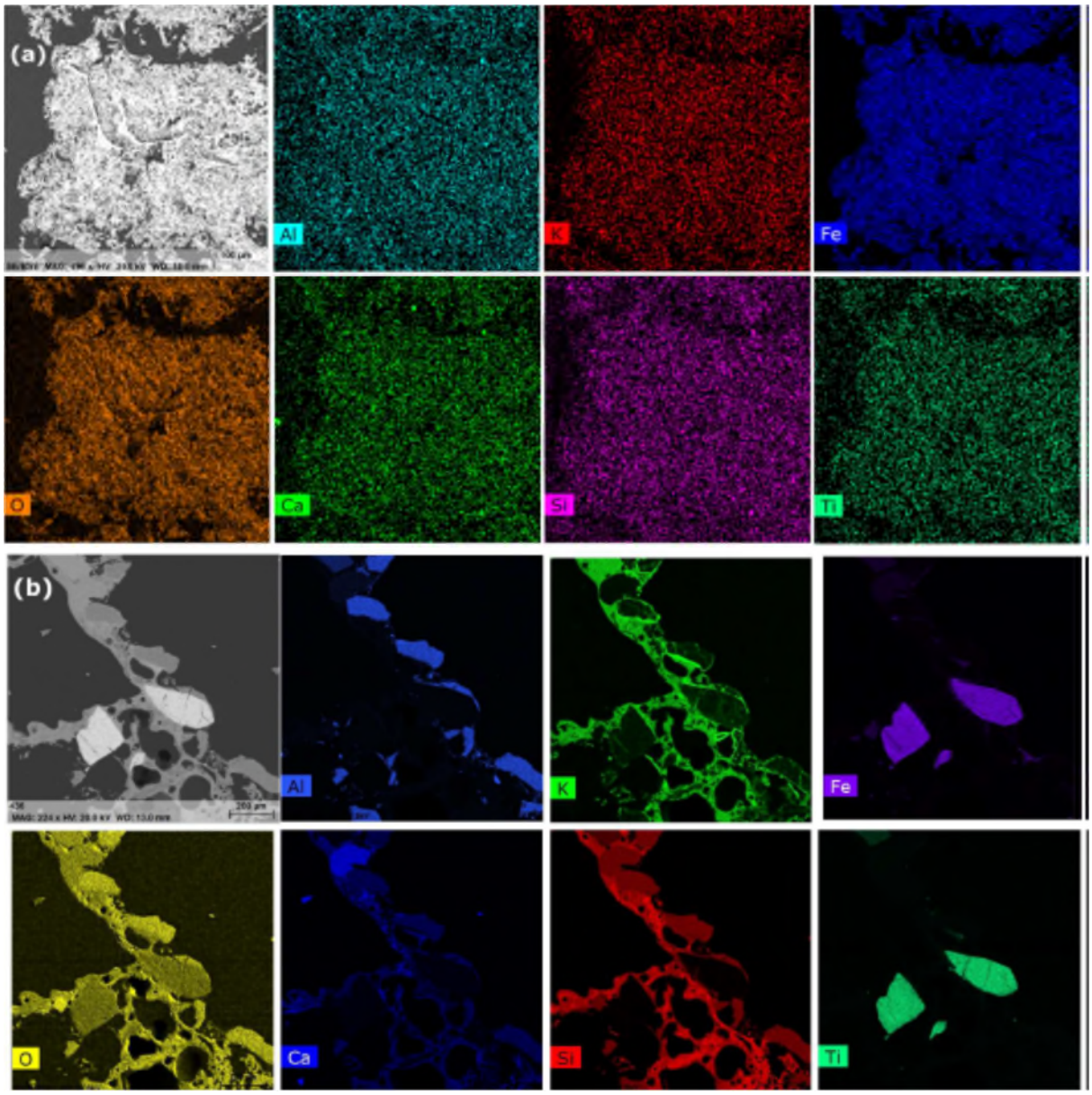

Figure 8. EDX elemental mapping of agglomerates samples from combustion of BC blended with STW at 40 wt% after 10 hours of operation, using (a) silica sand, and (b) ilmenite as bed material.

The results from EDX mapping analysis confirm the predominantly presence of Fe when silica sand was used as the bed material (Figure 8a). As for Ilmenite, K and Si were the dominant elements in the binder region, with a lesser intense presence of Al and Ca (Figure 8b). Because the reduced proportions of Fe and Ti in the binder compared to the ilmenite bed particles, only

those areas with the highest proportion were plotted. The presence of a Fe and Ti enriched layer on ilmenite particles surface was reported before by Lind et al. [34,51]. Nevertheless, studies with longer exposure times had reported the migration of Fe to the outer layer of the particles, indicating a segregation phenomenon of Fe from TiO_2, which could decrease the oxygen transport capacity of ilmenite [14], and the inward migration of K during biomass combustion [52]. During the relative short operating time (10 hours) of this study, no evidence of Fe segregation in the bed particles was observed. The distribution of O across the agglomerates (Fig. 8) can be considered an indication of the presence of studied elements in their oxidised forms.

3.4.2 X-Ray Fluorescence (XRF) Analysis of Cyclone Ash

Further analysis of the cyclone ash was performed by use of XRF to investigate the effect of bed material (silica sand and ilmenite) on the cyclone ash elemental composition. For comparison purpose, the cyclone ash from the combustion of pure coal with silica sand bed was included in the XRF analysis. The results shown in Figure 9 reveal a reduction in K and Ca contents in the cyclone ash when ilmenite was used as the bed material in comparison to silica sand. As expected, higher Fe and Ti contents were found in the cyclone ash when ilmenite was used. The lower content of K in the cyclone ash suggests the potential of ilmenite to capture alkali metals in the bed to form higher melting compounds. In addition, it confirms earlier findings from SEM-EDS analysis about K and Ca as the most active elements to interact with ilmenite. In comparison to the cyclone ash from coal combustion with silica sand bed, the cyclone ash of coal/biomass blend combustion revealed a lower content of Al, and a higher content of K. The lower content of Al is explained by the lower Al content in the fuel blend due to the negligible Al content in straw, which represent 40 wt% of the blend. The higher content of K in the fuel blend may suggest the formation of alkali-aluminosilicates structures

in the coating layers in the agglomerates, and this will be confirmed in the XRD analysis results to be presented in the next section. A higher K content in the ash can impose limitations regarding ash utilisation or increase disposal costs [53,54]. A much higher content of Ti was also found in the cyclone ash of coal/biomass blend combustion when ilmenite was used as the bed material. Heavy metals recovery from ash such as Ti is highly worthwhile due to the continually increasing consumption rates, the diversification in applications, and environmental risks associated with disposal and leaching of metals to surface and subsurface waters [55], [56].

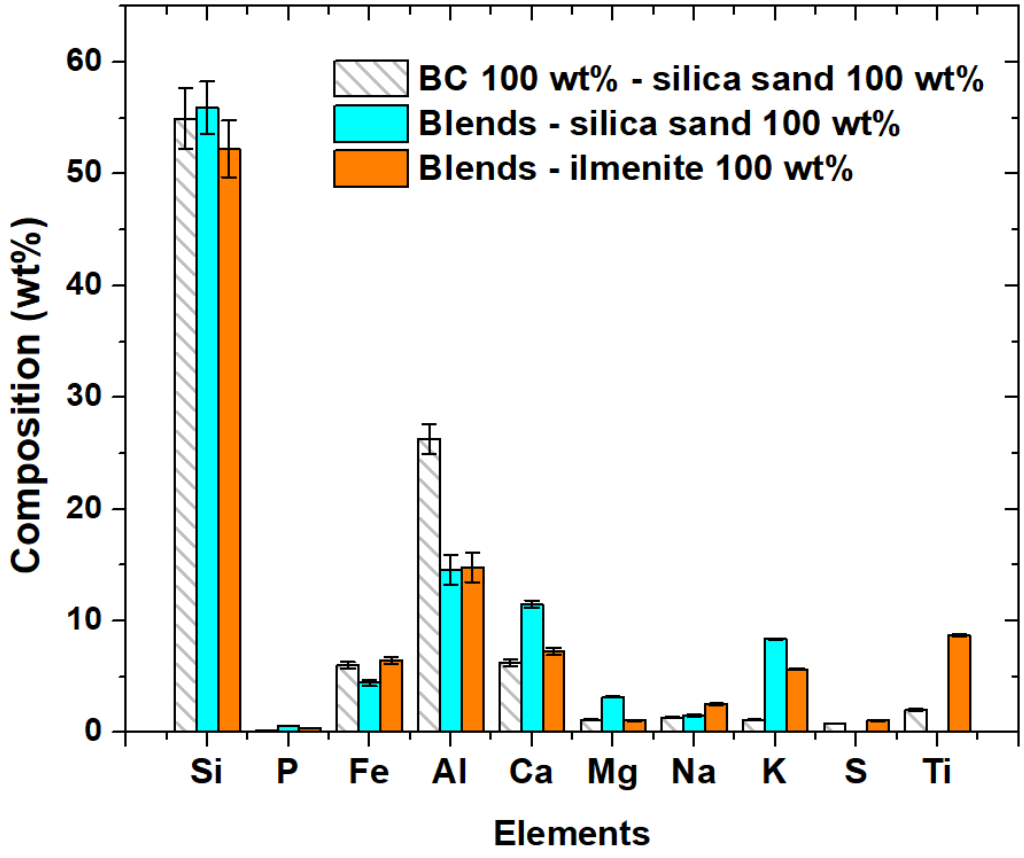

Figure 9. Elemental composition (XRF) of cyclone ash from combustion of BC blended with STW at 40 wt%, using silica sand and ilmenite as bed material (Bituminous coal (BC) at 100 wt% using silica sand was included for comparison purpose).

3.4.3 XRD Analysis of Agglomerates and Cyclone Ash

XRD patterns of agglomerates and cyclone ash using silica sand and ilmenite as bed materials are shown in Figures 10 and 11, respectively, while Table 4 presents the overview of the compounds found in agglomerates and cyclone ash that are shown in Figures 10 and 11. The analysis of agglomerates identified hematite (Fe_2O_3) as the unique crystalline phase when silica sand was used as the bed material. Other phases may exist in amorphous (glass) state of K_2O-SiO_2 in the agglomerates bound by fused, glassy materials, although such glassy materials would not be detected by XRD [57]. It is well known that silica minerals lose their crystallisation water at 300 - 1100 °C, resulting in structural collapse and consequent amorphisation in this temperature range [58]. However, this agrees with SEM/EDX results reported in Figure 7 with Si and K as the most common elements after Fe in the agglomerates found with the silica sand bed. Agglomerates bound by glassy materials have been identified as common in high silica biomass ash such as wheat straw [58]. In contrast, agglomerates found with ilmenite as the bed material showed a broad range of compounds, which was mainly attributed to the existence of impurities (see Table 2) in the mineral ore of ilmenite. Figure 10 showed SiO_2 to be the main phase with aluminosilicates, Ca-rich compounds, and iron-related phases in the agglomerates when 100 % ilmenite was used as the bed material. Furthermore, two potassium titanium oxides, KTi_8O_{16} and $K_2Ti_6O_{13}$, were identified when ilmenite was used as the bed material. These results are in line with previous findings reported by Corcoran et al. [25] and Wiinikka et al. [50]. The analysis of the cyclone ash samples in Figure 11 showed a variety of distinct peaks corresponding mainly to SiO_2, aluminosilicates, Ca-, Mg- K-bearing compounds. The presence of these compounds is consistent with the high concentration of silicon, potassium, aluminium, magnesium, iron, and calcium in the fuel blend ash as shown in Table 1. These results in Figures 10 and 11 suggest the potential of ilmenite as a K capturer in fluidised bed combustion.

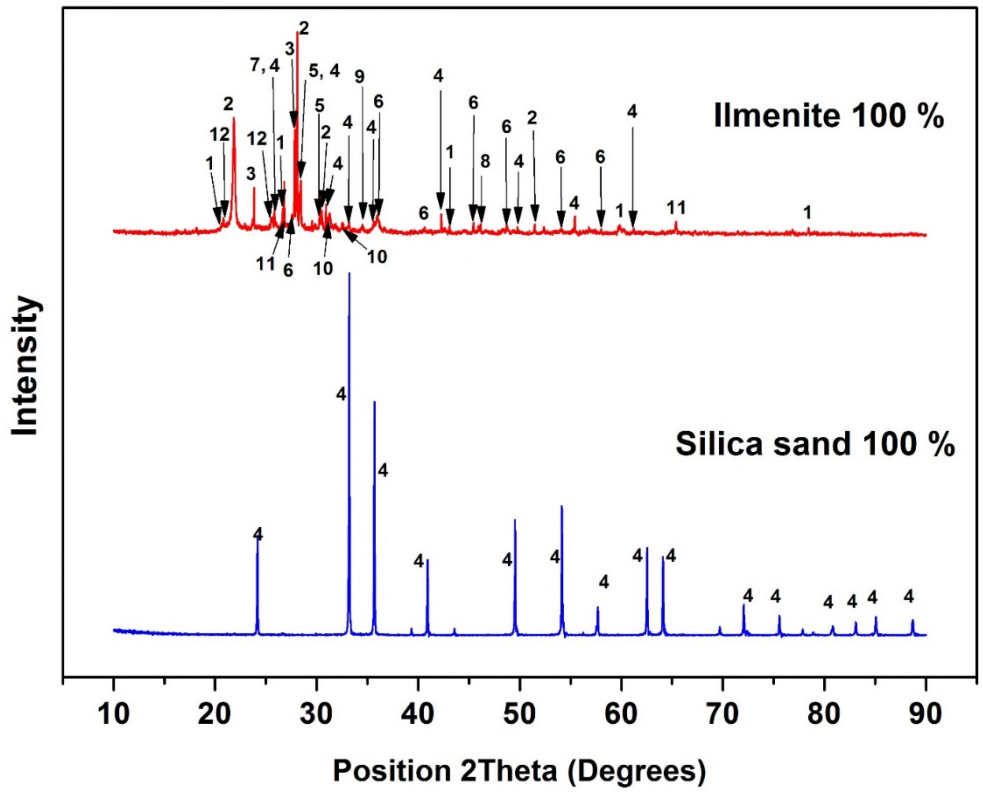

Figure 10. XRD patterns of bed agglomerates from bituminous coal (BC) blended with wheat straw (STW) at 40 wt%, using silica sand and ilmenite as bed material.

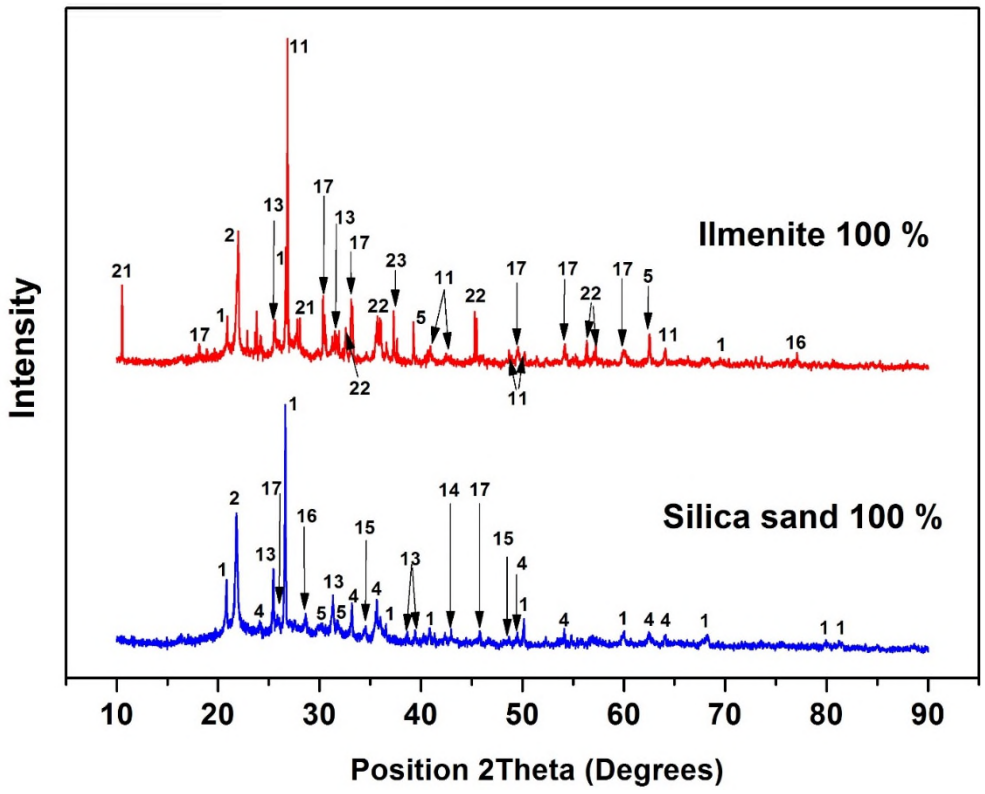

Figure 11. XRD patterns of cyclone ash from bituminous coal (BC) blended with wheat straw (STW) at 40 wt%, using silica sand and ilmenite as bed material.

Table 4. Overview of the compounds found in agglomerates and cyclone ash using silica sand and ilmenite as bed materials shown in Figures 9 and 10.

Component	Compound
(1)	Quartz
(2)	Cristobalite
(3)	$CaSiO_3$
(4)	Fe_2O_3 Hematite
(5)	$K_2CaP_2O_7$ Pyrophophite
(6)	KTi_8O_{16} Priderite
(7)	$FePO_4$ Rodolicoite
(8)	Fe_3O_4 Magnetite
(9)	Calcium aluminium silicate
(10)	$K_2Ti_6O_{13}$ Jeppeite
(11)	$CaAl_2(SiO_4)_2$ Anorthite
(12)	$KAlSi_3O_8$ orthoclase
(13)	$CaSO_4$ Anhydrite
(14)	MgO Periclase
(15)	MgS Niningerite
(16)	$K_{0.9}Na_{0.1}Cl$ Sylvite
(17)	Mullite
(18)	$AlPO_4$ Aluminium phosphate
(19)	$KCa_9Fe\ (PO_4)_7$ Potassium iron calcium phosphate
(20)	NaCl Halite
(21)	$K_{0.08}Mg_2Al_{4.17}Si_{4.83}O_{18}$ Potassium magnesium aluminium silicate
(22)	$CaAl_2SiO_6$ Kushiroite
(23)	Magnesium aluminium oxide
(24)	Calcium aluminium oxide $Ca_3\ (Al_2O_6)$
(25)	$CaSO_3$ calcium sulphite

The results from SEM/EDX, XRF, and XRD described above suggest that the difference in appearance observed between the agglomerated samples found with silica sand bed and ilmenite bed is more related to the difference in the variation of their chemical composition. Ilmenite as bed material led to the reduction of the agglomerates' size by forming high melting point compounds which hindered the K-rich molten substance attachment and resulted in heterogeneous coating layers in the agglomerates. These agglomerates appeared to be quite weak and were easily broken into smaller ones. In contrast, agglomerates from silica sand as

bed material showed a dense melt phase mainly composed of Fe with reduced amounts of Si, Al and K and closely connected structure. Therefore, ilmenite as the bed material can reduce the tendency of bed materials' agglomeration and defluidisation in comparison to silica sand bed.

3.5 Cracks and cracking layers in the bed particles

Ilmenite bed particles showed evidence of cracks. It has been reported as a consequence of mechanical and chemical stress, leading to attrition and fragmentation of bed materials [59]. Attrition has been identified as a limiting factor for the build-up of ash on ilmenite particles. It may cause the breakage of the formed layer, providing the possibility for Fe to migrate towards locations with high oxygen potential [44,52]. In contrast, finer particles of bed material can act as the cores for ash coagulation leading to an increase of the agglomeration tendency [20]. Cracks in the ilmenite bed particles may ease the diffusion of elements from the fuel ash into the particles [52].

Figure 12 shows the SEM/EDX elemental mapping of an ilmenite bed particle after 10 hours of operation to investigate the existence of cracks and the migration of elements into the particle. The results show Ca and K to be the most active ash elements to interact with ilmenite. Similar findings during combustion experiments in a CFB using wood as fuel and ilmenite as an additive were reported by Corcoran et al. [52]. The results in Figure 12 did not show interaction of the ash elements Si and Al. As expected, significant amounts of Fe and Ti were found across the particle. The results indicate that cracks in ilmenite particles help the migration of elements into the particles to form high melting temperature compounds.

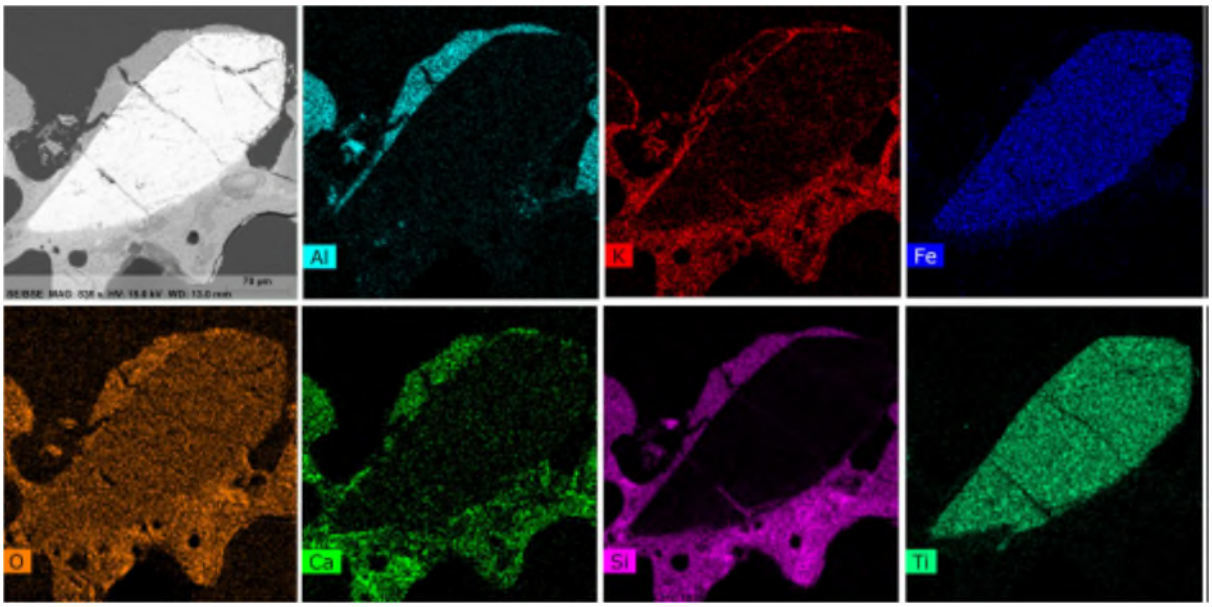

Figure 12. SEM/EDX elemental mapping illustration of cracks and the interaction of ash elements within the cross section of the ilmenite particle obtained from the combustion of BC blended with STW at 40 wt% after 10 hours of operation.

Conclusions

The effect of ilmenite on the gas emissions (CO, and NO_x), combustion performance and agglomeration tendency when used as alternative bed material under co-combustion conditions of coal blended with wheat straw pellets at 40 wt% was investigated in a 30 kWth pilot scale BFB combustor. The experiments were conducted at atmospheric pressure and 900 °C. For comparison purposes, silica sand was used as the baseline bed material. The agglomerates and the cyclone ash particles obtained from the combustion tests with different bed materials were characterised by means of XRF, XRD and SEM/EDX. The following conclusions can be drawn from the obtained experimental results:

1. Ilmenite leads to lower CO emissions and less efficiency loss when used as alternative bed material compared to the silica sand bed. This suggests ilmenite has the potential to decrease the excess air level needed to achieve complete combustion. However, ilmenite as the bed material resulted in an increase in NOx emissions under the

investigated conditions of this study, which means NOx control strategies such as air staging need to be adopted to control NOx emissions. It should be noted, due to the interest to investigate the agglomeration tendency at high operating temperatures and the limit of the experimental facility, the excess air level of this study was not optimised to the comparable values used in industrial-scale boilers.

2. Much less and smaller agglomerates were found when ilmenite was used as the bed material in comparison to silica sand. In addition, the agglomerates formed with the ilmenite bed appeared to be weak and easily broken.
3. The detailed analysis of the agglomerates and cyclone ash by means of XRF, XRD and SEM/EDX provided further evidence that ilmenite as bed material could reduce the tendency of agglomeration and defluidisation compared to the silica sand bed.

Acknowledgements

The research was supported by a Doctoral Research Fellowship from the Administrative Department of Science, Technology, and Innovation of Colombia (COLCIENCIAS) - Newton-Caldas Fund - '*Convocatoria 679 - 2014*'.

The authors would like to thank the Newark Factory of British Sugar plc (https://www.britishsugar.co.uk/), Agripellets (https://www.agripellets.com/), and Titania A/S (https://kronostio2.com/en/manufacturing-facilities/hauge-norway) for the support on the tested coal and silica sand, biomass fuel, and ilmenite, respectively, and the Nanoscale and Microscale Research Centre (nmRC) (https://www.nottingham.ac.uk/NMRC/) for providing access to instrumentation.

The authors would also like to acknowledge the help provided to the authors at the early stages of the reported research by Daniel Afilaka, who used to be a researcher at the University of Nottingham, Nick Smalley and James Edwards of British Sugar Plc.

References

[1] IEA, Global Energy Review 2019, 2020. https://www.iea.org/reports/global-energy-review-2019.

[2] IEA, Global Energy & CO_2 Status Report, 2019. www.iea.org/t&c/.

[3] IEA, Key Coal Trends, 2016.

[4] Agency for Natural Resources and Energy, Key World Energy statistics, IEA Int. Energy Agency. (2017). https://doi.org/10.1017/CBO9781107415324.004.

[5] T. Robl, A. Oberlink, R. Jones, Coal Combustion Products (CCPs), 2017.

[6] K. Sirisomboon, V.I. Kuprianov, Effects of fuel staging on the NO emission reduction during biomass-biomass co-combustion in a fluidized-bed combustor, Energy and Fuels. 31 (2017) 659–671. https://doi.org/10.1021/acs.energyfuels.6b02622.

[7] S.G. Sahu, N. Chakraborty, P. Sarkar, Coal-biomass co-combustion: An overview, Renew. Sustain. Energy Rev. 39 (2014) 575–586. https://doi.org/10.1016/j.rser.2014.07.106.

[8] P.J. Reddy, Clean Coal Technologies - for power generation, CRC Press, 2014.

[9] IRENA, Biomass Co- firing: Technology Brief, IEA-ETSAP IRENA©Technology Br. E21. (2013) 1–28. https://doi.org/IEA-ETSAP.

[10] P. Wang, H. Leion, H. Yang, Oxygen-Carrier-Aided Combustion in a Bench-Scale Fluidized Bed, Energy and Fuels. 31 (2017) 6463–6471. https://doi.org/10.1021/acs.energyfuels.7b00197.

[11] R. Hughes, R. Symonds, D. Lu, M. De, O. Loscertales, S. Champagne, Co-firing of Torrefied Biomass and Coal in Oxy - FBC with Ilmenite Bed Material, in: 75 IEA-FBC Meet., Skive, Denmark, 2017: pp. 1–23. http://www.ieafbc.org/past-events/75-iea-fbc-meeting/.

[12] M. Rydén, M. Hanning, L. Fredik, Improved combustion in fluidized bed with manganese ore as bed material, 2016. https://energiforsk.se/program/branslebaserad-el-och-varmeproduktion-sebra/rapporter/improved-combustion-in-fluidized-bed-with-manganese-ore-as-bed-material-2016-247/.

[13] H. Thunman, F. Lind, C. Breitholtz, N. Berguerand, M. Seemann, Using an oxygen-carrier as bed material for combustion of biomass in a 12-MWth circulating fluidized-bed boiler, Fuel. 113 (2013) 300–309. https://doi.org/10.1016/j.fuel.2013.05.073.

[14] Z. Yu, S. Yang, Q. Zhang, X. Hao, J. Zhao, Y. Yang, Y. Fang, G. Guan, Iron-based oxygen carriers in chemical looping conversions: A review, Carbon Resour. Convers. 2 (2018) 23–34. https://doi.org/10.1016/j.crcon.2018.11.004.

[15] J. Adánez, A. Abad, T. Mendiara, P. Gayán, L.F. de Diego, F. García-Labiano, Chemical looping combustion of solid fuels, Prog. Energy Combust. Sci. 65 (2018) 6–66. https://doi.org/10.1016/j.pecs.2017.07.005.

[16] H. Chen, Z. Zheng, Z. Chen, X.T. Bi, Reduction of hematite (Fe_2O_3) to metallic iron (Fe) by CO in a micro fluidized bed reaction analyzer: A multistep kinetics study, Powder Technol. 316 (2017) 410–420. https://doi.org/10.1016/j.powtec.2017.02.067.

[17] L. Chen, J. Bao, L. Kong, M. Combs, H.S. Nikolic, Z. Fan, K. Liu, Activation of ilmenite as an oxygen carrier for solid-fueled chemical looping combustion, Appl. Energy. 197 (2017) 40–51. https://doi.org/10.1016/j.apenergy.2017.03.127.

[18] I. Staničić, T. Mattisson, R. Backman, Y. Cao, M. Rydén, Oxygen carrier aided combustion (OCAC) of two waste fuels - Experimental and theoretical study of the interaction between ilmenite and zinc, copper and lead, Biomass and Bioenergy. 148 (2021). https://doi.org/10.1016/j.biombioe.2021.106060.

[19] R.W. Hughes, D.Y. Lu, R.T. Symonds, Improvement of Oxy-FBC Using Oxygen Carriers: Concept and Combustion Performance, Energy and Fuels. 31 (2017) 10101–

10115. https://doi.org/10.1021/acs.energyfuels.7b01556.

[20] H. Chi, M.A. Pans, C. Sun, H. Liu, An investigation of lime addition to fuel as a countermeasure to bed agglomeration for the combustion of non-woody biomass fuels in a 20kWth bubbling fluidised bed combustor, Fuel. 240 (2019) 349–361. https://doi.org/10.1016/j.fuel.2018.11.122.

[21] P. Teixeira, H. Lopes, I. Gulyurtlu, N. Lapa, P. Abelha, Evaluation of slagging and fouling tendency during biomass co-firing with coal in a fluidized bed, Biomass and Bioenergy. 39 (2012) 192–203. https://doi.org/10.1016/j.biombioe.2012.01.010.

[22] Y. Shao, C. (Charles) Xu, J. Zhu, F. Preto, J. Wang, G. Tourigny, C. Badour, H. Li, Ash Deposition during Co-firing Biomass and Coal in a Fluidized-Bed Combustor, Energy & Fuels. 24 (2010) 4681–4688. https://doi.org/10.1021/ef901228u.

[23] A. Khadilkar, P.L. Rozelle, S. V. Pisupati, Models of agglomerate growth in fluidized bed reactors: Critical review, status and applications, Powder Technol. 264 (2014) 216–228. https://doi.org/10.1016/j.powtec.2014.04.063.

[24] K.O. Davidsson, L.E. Åmand, B.M. Steenari, a. L. Elled, D. Eskilsson, B. Leckner, Countermeasures against alkali-related problems during combustion of biomass in a circulating fluidized bed boiler, Chem. Eng. Sci. 63 (2008) 5314–5329. https://doi.org/10.1016/j.ces.2008.07.012.

[25] A. Corcoran, P. Knutsson, F. Lind, H. Thunman, Mechanism for Migration and Layer Growth of Biomass Ash on Ilmenite Used for Oxygen Carrier Aided Combustion, Energy and Fuels. 32 (2018) 8845–8856. https://doi.org/10.1021/acs.energyfuels.8b01888.

[26] J. Gómez-Hernández, D. Serrano, A. Soria-Verdugo, S. Sánchez-Delgado, Agglomeration detection by pressure fluctuation analysis during Cynara cardunculus L. gasification in a fluidized bed, Chem. Eng. J. 284 (2016) 640–649.

https://doi.org/10.1016/j.cej.2015.09.044.

[27] Y. Niu, H. Tan, S. Hui, Ash-related issues during biomass combustion: Alkali-induced slagging, silicate melt-induced slagging (ash fusion), agglomeration, corrosion, ash utilization, and related countermeasures, Prog. Energy Combust. Sci. 52 (2016) 1–61. https://doi.org/10.1016/j.pecs.2015.09.003.

[28] A. Corcoran, J. Marinkovic, F. Lind, H. Thunman, P. Knutsson, M. Seemann, Ash Properties of Ilmenite Used as Bed Material for Combustion of Biomass in a Circulating Fluidized Bed Boiler, Energy & Fuels. 28 (2014) 7672–7679.

[29] D. Afilaka, Avoiding the sintering of coal fired shallow fluidised beds, Doctor of Engineering Thesis, University of Nottingham - UK, 2015.

[30] M. Rydén, M. Hanning, A. Corcoran, F. Lind, Oxygen Carrier Aided Combustion (OCAC) of Wood Chips in a Semi-Commercial Circulating Fluidized Bed Boiler Using Manganese Ore as Bed Material, Appl. Sci. 6 (2016) 347. https://doi.org/10.3390/app6110347.

[31] V.I. Kuprianov, R. Kaewklum, S. Chakritthakul, Effects of operating conditions and fuel properties on emission performance and combustion efficiency of a swirling fluidized-bed combustor fired with a biomass fuel, Energy. 36 (2011) 2038–2048. https://doi.org/10.1016/j.energy.2010.05.026.

[32] F. Guo, Z. Zhong, Co-combustion of anthracite coal and wood pellets: Thermodynamic analysis, combustion efficiency, pollutant emissions and ash slagging, Environ. Pollut. 239 (2018) 21–29. https://doi.org/10.1016/j.envpol.2018.04.004.

[33] A. Larsson, M. Israelsson, F. Lind, M. Seemann, H. Thunman, Using Ilmenite To Reduce the Tar Yield in a Dual Fluidized Bed Gasification System, Energy and Fuels. (2014).

[34] F. Lind, N. Berguerand, M. Seemann, H. Thunman, Ilmenite and Nickel as Catalysts

for Upgrading of Raw Gas Derived from Biomass Gasification, Energy and Fuels. (2013).

[35] E. Karampinis, P. Grammelis, M. Agraniotis, I. Violidakis, E. Kakaras, Co-Firing of Biomass with Coal in Thermal Power Plants: Technology Schemes, Impacts, and Future Perspectives, WIREs Energy Environ. 3 (2014) 384–399. https://doi.org/10.1002/wene.100.

[36] A. Tchapda, S. Pisupati, A Review of Thermal Co-Conversion of Coal and Biomass/Waste, Energies. 7 (2014) 1098–1148. https://doi.org/10.3390/en7031098.

[37] P. Glarborg, A.D. Jensen, J.E. Johnsson, Fuel nitrogen conversion in solid fuel fired systems, Prog. Energy Combust. Sci. 29 (2003) 89–113. https://doi.org/10.1016/S0360-1285(02)00031-X.

[38] R. Nersesian, Energy Economics, markets, history and policies, Routledge, 2016.

[39] C.E. Baukal, The John Zink Hamworthy Combustion Handbook, Second Edition: Volume 3 – Applications, 2nd ed., 2013. https://doi.org/10.1201/b12975-4.

[40] E. Dahlquist, Technologies for Converting Biomass to useful Energy, CRC Press, 2013.

[41] J. Xie, X. Yang, L. Zhang, T. Ding, W. Song, W. Lin, Emissions of SO_2, NO and N_2O in a circulating fluidized bed combustor during co-firing coal and biomass, J. Environ. Sci. 19 (2007) 109–116. https://doi.org/10.1016/S1001-0742(07)60018-7.

[42] F. Normann, A.O. Wismer, C.R. Müller, H. Leion, Oxidation of ammonia by iron, manganese and nickel oxides – Implications on NOx formation in chemical-looping combustion, Fuel. 240 (2019) 57–63. https://doi.org/10.1016/j.fuel.2018.11.121.

[43] F. Scala, R. Chirone, An SEM/EDX study of bed agglomerates formed during fluidized bed combustion of three biomass fuels, Biomass and Bioenergy. 32 (2008) 252–266. https://doi.org/10.1016/j.biombioe.2007.09.009.

[44] J. Adánez, A. Abad, F. Garcia-Labiano, P. Gayan, L.F. De Diego, Progress in chemical-looping combustion and reforming technologies, Prog. Energy Combust. Sci. 38 (2012) 215–282. https://doi.org/10.1016/j.pecs.2011.09.001.

[45] R.C. Brown, M.R. Dawson, J.L. Smeenk, Bed Material Agglomeration During Fluidized Bed Combustion, Iowa State University-U.S. Department of Energy - DOE/PC/92530-T14, 1996.

[46] D. Spreitzer, J. Schenk, Reduction of Iron Oxides with Hydrogen—A Review, Steel Res. Int. 90 (2019). https://doi.org/10.1002/srin.201900108.

[47] L. Guo, S. Zhong, Q. Bao, J. Gao, Z. Guo, Nucleation and growth of iron whiskers during gaseous reduction of hematite iron ore fines, Metals (Basel). 9 (2019). https://doi.org/10.3390/met9070750.

[48] S. V. Vassilev, D. Baxter, C.G. Vassileva, An overview of the behaviour of biomass during combustion: Part II. Ash fusion and ash formation mechanisms of biomass types, Fuel. 117 (2014) 152–183. https://doi.org/10.1016/j.fuel.2013.09.024.

[49] P. Basu, Combustion and gasification in fluidized beds, CRC Press, 2006.

[50] H. Wiinikka, C. Grönberg, O. Öhrman, D. Boström, Influence of TiO_2 Additive on Vaporization of Potassium during Straw Combustion, Energy & Fuels. 23 (2009) 5367–5374. https://doi.org/10.1021/ef900544z.

[51] M. Zevenhoven, C. Sevonius, P. Salminen, D. Lindberg, A. Brink, P. Yrjas, L. Hupa, Defluidization of the oxygen carrier ilmenite – Laboratory experiments with potassium salts, Energy. 148 (2018) 930–940. https://doi.org/10.1016/j.energy.2018.01.184.

[52] A. Corcoran, P. Knutsson, F. Lind, H. Thunman, Comparing the structural development of sand and rock ilmenite during long-term exposure in a biomass fired 12 MWth CFB-boiler, Fuel Process. Technol. 171 (2018) 39–44. https://doi.org/10.1016/j.fuproc.2017.11.004.

[53] A. Fuller, J. Maier, E. Karampinis, J. Kalivodova, P. Grammelis, E. Kakaras, G. Scheffknecht, Fly ash formation and characteristics from (co-)Combustion of an herbaceous biomass and a Greek lignite (Low-Rank Coal) in a pulverized fuel pilot-scale test facility, Energies. 11 (2018). https://doi.org/10.3390/en11061581.

[54] N. Cheremisinoff, Clean Electricity Through Advanced Coal Technologies, Elsevier Inc., 2012.

[55] P.K. Sahoo, K. Kim, M.A. Powell, S.M. Equeenuddin, Recovery of metals and other beneficial products from coal fly ash: a sustainable approach for fly ash management, Int. J. Coal Sci. Technol. 3 (2016) 267–283. https://doi.org/10.1007/s40789-016-0141-2.

[56] H. Hasegawa, I.M.M. Rahman, Y. Egawa, H. Sawai, Z.A. Begum, T. Maki, S. Mizutani, Recovery of the rare metals from various waste ashes with the aid of temperature and ultrasound irradiation using chelants, Water. Air. Soil Pollut. 225 (2014). https://doi.org/10.1007/s11270-014-2112-9.

[57] X. Ma, F. Li, M. Ma, Y. Fang, Investigation on Blended Ash Fusibility Characteristics of Biomass and Coal with High Silica–Alumina, Energy & Fuels. 31 (2017) 7941–7951. https://doi.org/10.1021/acs.energyfuels.7b01070.

[58] S. V. Vassilev, D. Baxter, L.K. Andersen, C.G. Vassileva, An overview of the composition and application of biomass ash. Part 1. Phase-mineral and chemical composition and classification, Fuel. 105 (2013) 40–76. https://doi.org/10.1016/j.fuel.2012.09.041.

[59] P. Knutsson, C. Linderholm, Characterization of ilmenite used as oxygen carrier in a 100 kW chemical-looping combustor for solid fuels, Appl. Energy. 157 (2015) 368–373. https://doi.org/10.1016/j.apenergy.2015.05.122.

Supplementary Material

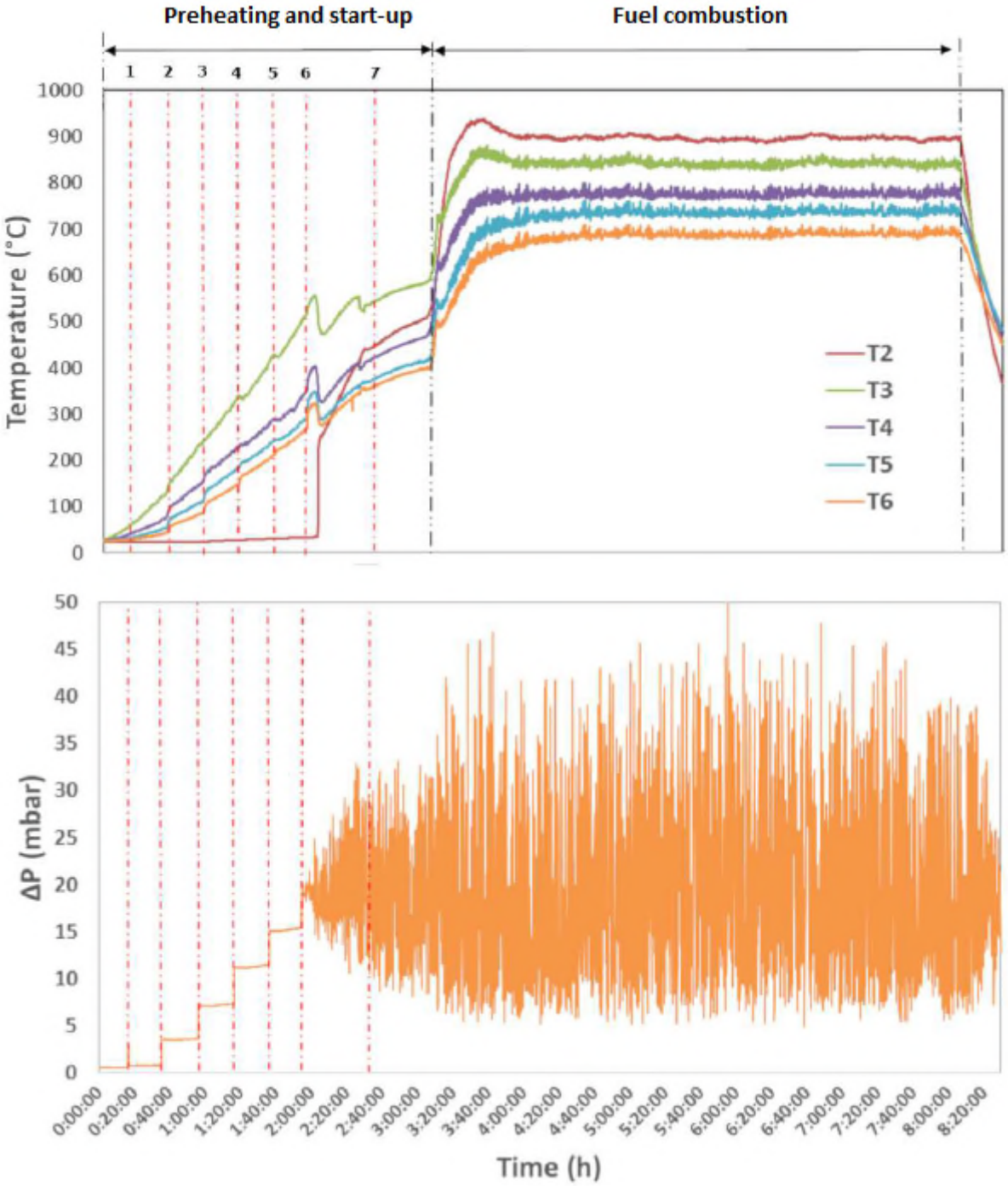

S1. Typical temperature profile (top) and pressure differential profile (bottom) across the 30kWth bubbling fluidised bed combustor using ilmenite as bed material - bed temperature, T_2 = 901 °C.

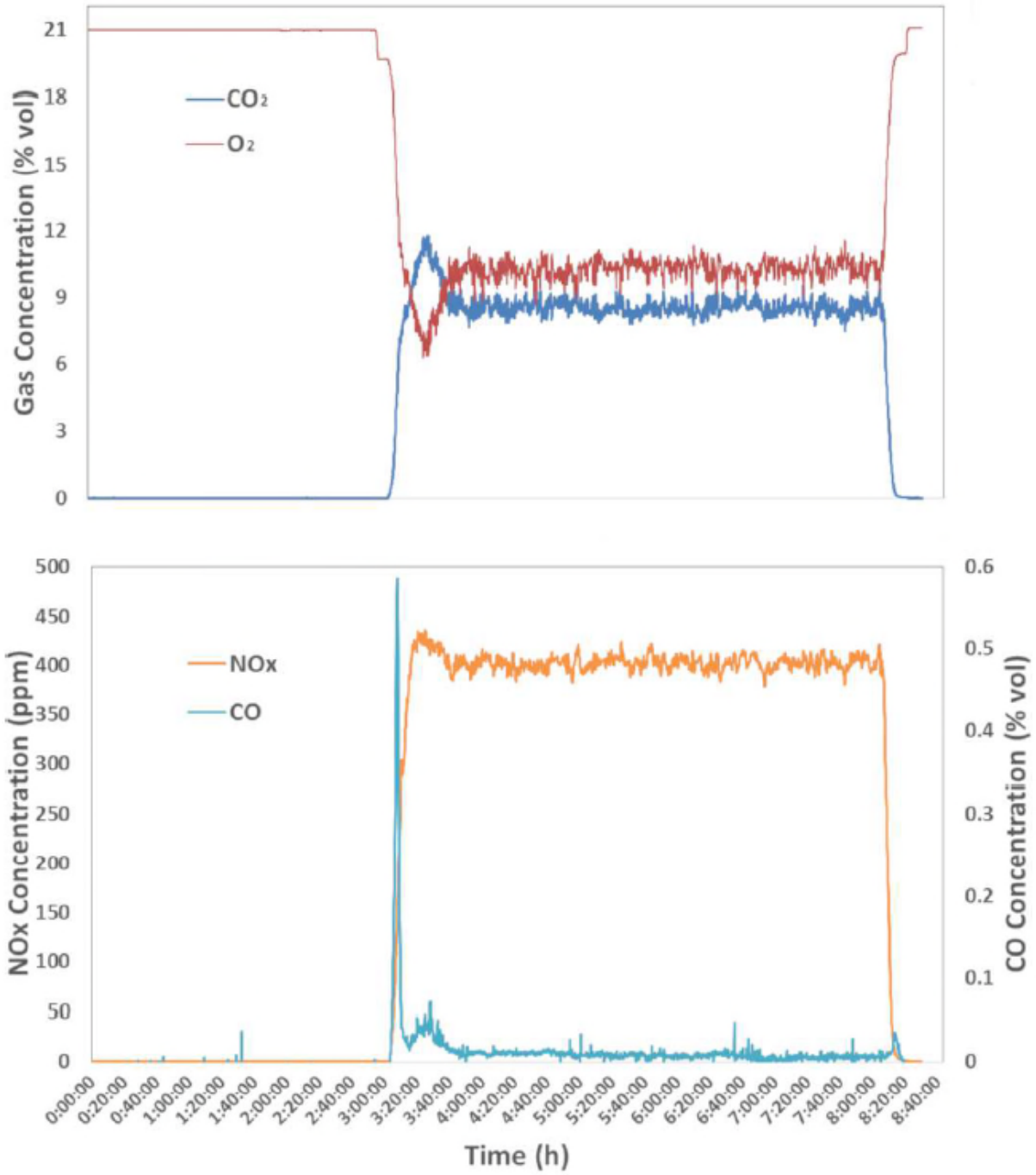

S2. Flue gas composition, CO_2 and O_2 concentration (top), and NOx and CO concentration (bottom) at the outlet of the 30kWth bubbling fluidised bed combustor using ilmenite as the bed material.